
Numerical Heat Transfer, Part A: Applications: An International Journal of Computation and Methodology
Publication details, including instructions for authors and subscription information:
http://www.tandfonline.com/loi/unht20

# NUMERICAL INVESTIGATION OF HEAT TRANSFER OF A HEATED CHANNEL WITH AN OSCILLATING CYLINDER

Wu-Shung Fu [a] & Bao-Hong Tong [a]
[a] Department of Mechanical Engineering, National Chiao Tung University,Taiwan, Republic of China
Published online: 30 Nov 2010.

To cite this article: Wu-Shung Fu & Bao-Hong Tong (2003) NUMERICAL INVESTIGATION OF HEAT TRANSFER OF A HEATED CHANNEL WITH AN OSCILLATING CYLINDER, Numerical Heat Transfer, Part A: Applications: An International Journal of Computation and Methodology, 43:6, 639-658, DOI: 10.1080/10407780307348

To link to this article: http://dx.doi.org/10.1080/10407780307348

Numerical Heat Transfer, Part A, 43: 639–658, 2003

1040-7782/03 $12.00 + .00
DOI: 10.1080/10407780390123005

Taylor & Francis
Taylor & Francis Group

# NUMERICAL INVESTIGATION OF HEAT TRANSFER OF A HEATED CHANNEL WITH AN OSCILLATING CYLINDER

*Wu-Shung Fu and Bao-Hong Tong*
*Department of Mechanical Engineering,*
*National Chiao Tung University,*
*Taiwan, Republic of China*

***A numerical simulation is performed to study the influence on the heat transfer rate of the heated wall in the channel with an oscillating cylinder. An arbitrary Lagrangian-Eulerian kinematic description method is adopted to describe the flow and thermal fields. A penalty consistent finite-element formulation is applied to solve the governing equations. The effects of Reynolds number, oscillating amplitude, oscillating frequency, eccentric ratio, and blockage on the heat transfer characteristics of the heated wall are examined. The results show that not only the region relating to heat transfer is enlarged substantially, but also that the heat transfer rate of this region is enhanced remarkably.***



## INTRODUCTION

The problem of force convection in a channel is of practical importance and widely considered in the design of devices such as heat exchangers, advanced gas-cooled reactor fuel elements, and internal cooling passages of gas turbines. Therefore, there is an urgent need to improve performance of the channel heat transfer rate.

A summary of the literature on heat transfer in a laminar duct flow was brought together in a book by Shah and London [1]. It indicated analytical solutions for laminar fluid flow and forced-convection heat transfer in many passage geometries. Furthermore, numerous methods have been proposed to enhance heat transfer rate with both passive and active methods. A channel or pipe installed with ribs is often used to enhance the heat transfer rate. Many studies, such as those of Sparrow et al. [2] and Bergeles and Athanassiadis [3], investigated this issue, and the results showed that the ribs disturbed the flow field and enlarged the heat transfer area to cause the increment of the heat transfer rate. Similar to the effect of the rib, the turbulence promoter, which can contract flow space and disturb fluid flow, is also widely used to improve heat transfer of a channel. Liou et al. [4–6] did a series of

Received 11 April 2002; accepted 7 August 2002.
Support of this work by the National Science Council of Taiwan, Republic of China, under contract NSC89-2212-E009-019 is gratefully acknowledged.
Address correspondence to Dr. Wu-Shung Fu, National Chiao Tung University, Department of Mechanical Engineering, 1001 Ta Hsueh Road, Hsinchu, Taiwan 30056, Republic of China. E-mail: wsfu@cc.nctu.edu.tw

## NOMENCLATURE

| | | | |
|---|---|---|---|
| $d$ | diameter of cylinder, m | | directions ($U = u/u_0$, $V = v/u_0$) |
| $f$ | friction factor | $\hat{v}$ | mesh velocity in $y$-direction, $m/s$ |
| $f_c$ | oscillating frequency of cylinder, $s^{-1}$ | $v_c$ | oscillating velocity of cylinder, $m/s$ |
| $f_e$ | friction factor in empty channel | $v_m$ | maximum oscillating velocity of cylinder, $m/s$ |
| $F_c$ | dimensionless oscillating frequency of cylinder ($= f_c d/u_c$) | $\hat{V}$ | dimensionless mesh velocity in $Y$-direction ($= \hat{v}/u_0$) |
| $h_c$ | distance from bottom side to center of cylinder, m | $V_c$ | dimensionless oscillating velocity of cylinder ($= \upsilon_c/u_0$) |
| $he$ | height of the channel, m | $V_m$ | dimensionless maximum oscillating velocity of cylinder ($= v_m/u_0$) |
| $k$ | thermal conductivity | $w$ | length of channel, m |
| $l_c$ | oscillating amplitude of cylinder, m | $w_1$ | length of adiabatic region before cylinder, m |
| $L_c$ | dimensionless oscillating amplitude ($= l_c/d$) | $w_2$ | length of high-temperature region before cylinder, m |
| $\overline{\mathrm{Nu}}$ | periodic-averaged Nusselt number | $w_3$ | length of high-temperature region behind cylinder, m |
| $\overline{\mathrm{Nu}}_e$ | average Nusselt number of overall heated surface in the empty channel | $w_4$ | dimensional length of adiabatic region behind cylinder, m |
| $\mathrm{Nu}_X$ | local Nusselt number | $x, y$ | dimensional Cartesian coordinates, m |
| $\mathrm{Nu}_{(X_1)-(X_2)}$ | average Nusselt number from $X_1$ to $X_2$ | $X, Y$ | dimensionless Cartesian coordinates ($X = x/he$, $Y = y/he$) |
| $p$ | dimensional pressure, $N/m^2$ | $\alpha$ | thermal diffusivity, $m^2/s$ |
| $p_\infty$ | reference pressure, $N/m^2$ | $\theta$ | dimensionless temperature $= (T - T_0)/(T_c - T_0)$ |
| $P$ | dimensionless pressure $= (p - p_\infty)/\rho u_0^2$ | $\theta_{mX}$ | dimensionless local mean temperature |
| Pr | Prandtl number ($= \upsilon/\alpha$) | $\lambda$ | penalty parameter |
| $q''_w$ | heat transfer rate from heated wall | $\nu$ | kinematic viscosity, $m^2/s$ |
| $r$ | radius of cylinder, m | $\rho$ | density, $kg/m^3$ |
| $R$ | dimensionless radial coordinate ($= r/he$) | $\tau$ | dimensionless time ($= tu_0/he$) |
| Re | Reynolds number ($= u_0 he/v$) | $\tau_p$ | dimensionless time of one oscillating cycle |
| $t$ | time, s | $\Phi$ | computational variables |
| $T$ | temperature, K | $\Psi$ | dimensionless stream function |
| $T_H$ | temperature of high-temperature region, K | **Other** | |
| $T_{mx}$ | local mean temperature, K | $\|$ | absolute value |
| $T_0$ | temperature of inlet fluid, K | | |
| $u, v$ | velocities in $x$ and $y$ directions, $m/s$ | | |
| $u_0$ | velocities of inlet fluid, $m/s$ | | |
| $U, V$ | dimensionless velocities in $X$ and $Y$ | | |

numerical and experimental researches on the turbulent flows in a channel with turbulence promoters, and the results showed that the pitch ratio, Reynolds number, and eccentricity ratio affected the phenomena of separation, reattachment, and heat transfer rate. Amon et al. [7, 8] studied self-sustained oscillatory flows in communicating channels. The results indicated the self-sustained oscillation that resulted in very well-mixed flows. On an equal pumping power basis, the heat transfer in communicating channels flows was higher than that in a flat channel flow. Lin and Hung [9] studied the transient forced-convection heat transfer in a vertical rib-heated channel with a turbulence promoter, and found that the utilization of a turbulence promoter could effectively improve the heat transfer performance in the fully developed region. Hwang [10] conducted an experimental investigation of heat transfer

in a rectangular duct of which one wall was roughened by slit and solid ribs. The results showed that the slit ribs provided better thermal performance under constant friction power. Wu and Perng [11] did a numerical investigation of heat transfer enhancement in a horizontal block-heated channel with installation of an oblique plate. The maximum increase of average Nusselt number was 39.5% when the oblique angle was $\pi/3$.

From the above literature, due to the existence of the ribs, the phenomena of separation and reattachment occurred in the flow field, which caused the heat transfer in the circulation zone to be complex and small. Then, the increment of heat transfer rate in the channel flow seems to have been limited by using the above passive methods. Therefore, Fu et al. [12] adopted the active method of using a moving block on a heated surface to improve the heat transfer rate in a channel. In their study, the maximum heat transfer rate increment is about 98%. However, the method is hard to use in a ribbed channel. For improving the heat transfer rate of the heated surface in the channel, an effective method is proposed in this study and the method is to utilize an oscillating cylinder in the channel to cause the occurrence of flow vibration, which can enhance the heat transfer rate.

There have been many numerical and experimental studies [13–15] to investigate flow passing an oscillating cylinder. The phenomena indicated that significant vibration occurred in the vortex flow structure in the lock-on frequency. Cheng et al. [16, 17], Karanth et al. [18], and Gau et al. [19] investigated heat transfer around a heated oscillating circular cylinder using experimental and numerical methods. The results found that the enhancement of heat transfer was proportional to the magnitude of the oscillating frequency and amplitude of the circular cylinder and the heat transfer increased remarkably as the flow approached the lock-in regime. Park and Gharib [20] studied heat convection in stationary and oscillating circular cylinders in cross-flow by an experimental method; the increase in heat transfer rate was found to correlate inversely with distance at which vortices roll up behind the cylinder.

Most of the above research focused on the flow vibration induced by an oscillating cylinder set in an infinite space and the heat transfer rate of the oscillating cylinder itself. However, investigation of the relationships with the oscillating cylinder set in the channel and the heat transfer around the walls of the channel is rare. The subject of the present work is therefore to investigate the influence of flow passing over an oscillating cylinder on the heated surface in the channel.

The subject mentioned above is a kind of moving-boundary problem, and the arbitrary Lagrangian Eulerian (ALE) method modified by Fu and Yang [21] is suitably adopted to solve this problem. The heat transfer characteristics along the heated surface are presented in detail. The effects of Reynolds number, oscillating amplitude, and oscillating frequency on the flow structures and heat transfer characteristics are investigated.

## PHYSICAL MODEL

The physical model used in this study is shown in Figure 1. A two-dimensional channel with height $he$ and length $w$ is used to simulate this problem. An insulated cylinder of diameter $d$ is set within the channel. The distances from the inlet and outlet of the channel to the center of the cylinder are $w_1 + w_2$ and $w_3 + w_4$,

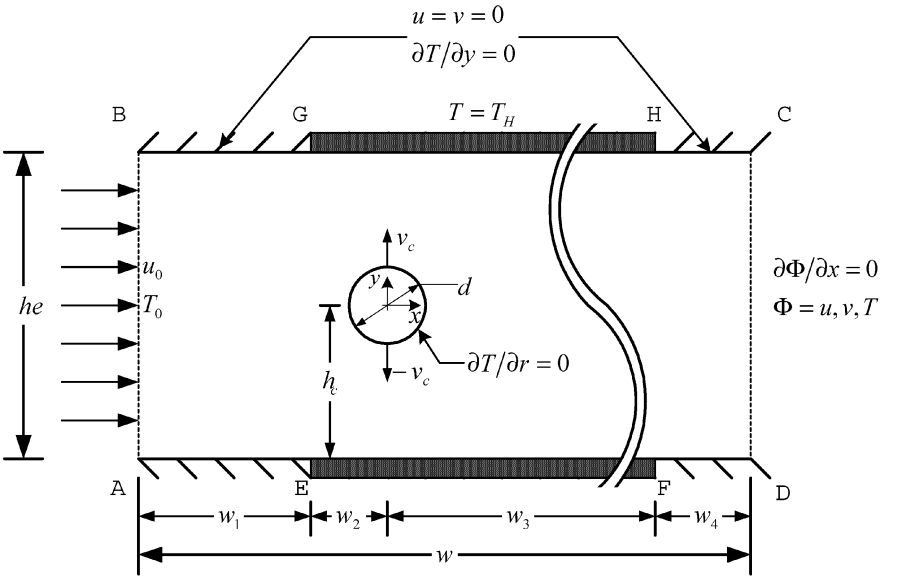


**Figure 1.** Physical model.

respectively. The inlet velocity $u_0$ and temperature $T_0$ of the fluid are uniform. The temperature of the heated surfaces EF, GH with length $w_2 + w_3$ is $T_H$, which is higher than $T_0$. The other surfaces of the channel (surfaces AG, HD, BE, and FC) are insulated. Initially, the cylinder is stationary at the position of the center of the channel and the fluid flows steadily. The distance from the wall of the channel to the center of the cylinder is $h_c$. As the time $t > 0$, the cylinder is in oscillating motion normal to the inlet flow with amplitude $l_c$. The oscillating velocity of the cylinder is $v_c = 2\pi l_c \cos(2\pi f_c t)$. The behavior of the oscillating cylinder and the flow are then affected mutually, and the variations of the flow field become time-dependent and are classified into a class of moving-boundary problem. As a result, the ALE method is properly utilized to analyze this problem.

To facilitate the analysis, the following assumptions are made.

1. The fluid is air and the flow field is two-dimensional, incompressible, and laminar.
2. The fluid properties are constant and the effect of the gravity is neglected.
3. The no-slip condition is held on the interfaces between the fluid and cylinder.

Based on the characteristic scales of $w$, $u_0$, $\rho u_0^2$, and $T_0$, the dimensionless variables are defined as follows:

$$X = \frac{x}{he} \qquad Y = \frac{y}{he} \qquad U = \frac{u}{u_0} \qquad V = \frac{v}{u_0} \qquad \hat{V} = \frac{\hat{v}}{u_0}$$
$$V_c = \frac{v_c}{u_0} \qquad L_c = \frac{l_c}{he} \qquad H_c = \frac{h_c}{he} \qquad F_c = \frac{f_c d}{u_0} \qquad P = \frac{p - p_\infty}{\rho u_0^2} \tag{1}$$
$$\tau = \frac{t u_0}{he} \qquad \theta = \frac{T - T_0}{T_H - T_0} \qquad \mathrm{Re} = \frac{u_0 he}{\upsilon} \qquad \mathrm{Pr} = \frac{\upsilon}{\alpha}$$

where $\hat{v}$ is the mesh velocity, and $v_c$, $f_c$, $h_c$, and $l_c$ are the oscillating velocity, the oscillating frequency, the position, and the oscillating amplitude of the cylinder, respectively.

According to the above assumptions and dimensionless variables, the dimensionless ALE governing equations are expressed as the following equations.

Continuity equation:

$$\frac{\partial U}{\partial X}+\frac{\partial V}{\partial Y}=0, \tag{2}$$

Momentum equation:

$$\frac{\partial U}{\partial \tau}+U\frac{\partial U}{\partial X}+(V-\hat{V})\frac{\partial U}{\partial Y}=-\frac{\partial P}{\partial X}+\frac{1}{\mathrm{Re}}\left(\frac{\partial^2 U}{\partial X^2}+\frac{\partial^2 U}{\partial Y^2}\right) \tag{3}$$

$$\frac{\partial V}{\partial \tau}+U\frac{\partial V}{\partial X}+(V-\hat{V})\frac{\partial V}{\partial Y}=-\frac{\partial P}{\partial Y}+\frac{1}{\mathrm{Re}}\left(\frac{\partial^2 V}{\partial X^2}+\frac{\partial^2 V}{\partial Y^2}\right) \tag{4}$$

Energy equation:

$$\frac{\partial \theta}{\partial \tau}+U\frac{\partial \theta}{\partial X}+(V-\hat{V})\frac{\partial \theta}{\partial Y}=-\frac{1}{\mathrm{Re}\,\mathrm{Pr}}\left(\frac{\partial^2 \theta}{\partial X^2}+\frac{\partial^2 \theta}{\partial Y^2}\right) \tag{5}$$

As the time $\tau > 0$, the boundary conditions are as follows.

On the inlet surface AB:

$$U=1 \qquad V=0 \qquad \theta=0 \tag{6}$$

On the walls BG, HC, AE, and FD:

$$U=0 \qquad V=0 \qquad \frac{\partial \theta}{\partial Y}=0 \tag{7}$$

On the walls EF and GH:

$$U=0 \qquad V=0 \qquad \theta=1 \tag{8}$$

On the outlet surface CD:

$$\frac{\partial U}{\partial X}=0 \qquad \frac{\partial V}{\partial X}=0 \qquad \frac{\partial \theta}{\partial X}=0 \tag{9}$$

On the interfaces between the fluid and cylinder:

$$U=0 \qquad V=V_c \qquad \frac{\partial \theta}{\partial R}=0 \tag{10}$$

## NUMERICAL METHOD

The governing equations and boundary conditions are solved through the Galerkin finite-element formulation, and a backward scheme is adopted to deal with the time terms of the governing equations. The pressure is eliminated from the governing equations using the consistent penalty method. The velocity and temperature terms are expressed as quadrilateral elements and eight-node quadratic Lagrangian interpolation functions. The Newton–Raphson iteration algorithm is utilized to simplify the nonlinear terms in the momentum equations. The discretization processes for the governing equations are similar to the ones used in Fu et al. [21]. Then, the momentum equations (3) and (4) can be expressed as the following matrix form:

$$\sum_{1}^{n_e}([A]^{(e)} + [K]^{(e)} + \lambda[L]^{(e)})\{q\}^{(e)}_{\tau+\Delta\tau} = \sum_{1}^{n_e}\{f\}^{(e)} \tag{11}$$

where

$$(\{q\}^{(e)}_{\tau+\Delta\tau})^T = \langle U_1, U_2, \ldots, U_8, V_1, V_2, \ldots, V_8\rangle^{m+1}_{\tau+\Delta\tau} \tag{12}$$

$[A]^{(e)}$ includes the $m$th iteration values of $U$ and $V$ at time $\tau + \Delta\tau$.
$[K]^{(e)}$ includes the shape function, $\hat{V}$, and time differential terms.
$[L]^{(e)}$ includes the plenty function.
$[f]^{(e)}$ includes the known values of $U$ and $V$ at time $\tau$ and $m$th-iteration values of $U$ and $V$ at time $\tau + \Delta\tau$.

The energy equation (5) can be expressed as the following matrix form:

$$\sum_{1}^{n_e}([M]^{(e)} + [Z]^{(e)})\{c\}^{(e)}_{\tau+\Delta\tau} = \sum_{1}^{n_e}\{r\}^{(e)} \tag{13}$$

where

$$(\{c\}^{(e)}_{\tau+\Delta\tau})^T = \langle \theta_1, \theta_2, \ldots, \theta_8\rangle_{\tau+\Delta\tau} \tag{14}$$

$[M]^{(e)}$ includes the values of $U$ and $V$ at time $\tau + \Delta\tau$.
$[Z]^{(e)}$ includes the shape function, $\hat{V}$, and time differential terms.
$[r]^{(e)}$ includes the known values of $\theta$ at time $\tau$.

In Eqs. (11) and (13), Gaussian quadrature procedure are conveniently used to execute the numerical integration. The terms with the penalty parameter $\lambda$ are integrated by $2 \times 2$ Gaussian quadrature, and the other terms are integrated by $3 \times 3$ Gaussian quadrature. The value of penalty parameter $\lambda$ used in this study is $10^6$. The frontal method solver is applied to solve Eqs. (10) and (12). The mesh velocity $\hat{V}$ is linearly distributed and inversely proportional to the distance between the nodes of the computational elements and cylinder.

A brief outline of the solution procedures is as follows.

1. Determine the optimal mesh distribution and number of the elements and nodes.
2. Solve for the values of $U$, $V$, and $\theta$ at steady state and regard them as the initial values.
3. Determine the time step $\Delta\tau$ and the mesh velocity $\hat{V}$ of the computational meshes.
4. Update the coordinates of the nodes and examine the determinant of the Jacobian transformation matrix to ensure that the one-to-one mapping is satisfied during the Gaussian quadrature numerical integration.
5. Solve Eq. (11) until the following criterion for convergence is satisfied:

$$\left|\frac{\Phi^{m+1}-\Phi^{m}}{\Phi^{m+1}}\right|_{\tau+\Delta\tau} < 10^{-3} \qquad \text{where } \Phi = U \text{ and } V \tag{15}$$

   and substitute the $U$ and $V$ into Eq. (12) to obtain $\theta$.
6. Continue with the next time-step calculation until periodic solutions are attained.

## RESULTS AND DISCUSSION

The working fluid is air with $\mathrm{Pr} = 0.71$. The main parameters of Reynolds number Re, oscillating amplitude $L_c$, and oscillating frequency $F_c$ are examined, and the combinations of these parameters are tabulated in Table 1.

In the channel, the thermal boundary layer grows gradually in the downstream direction. To describe the wall heat transfer in the channel region realistically, it is necessary to define the local mean temperature $T_{mx}$ of the stream as the environmental temperature:

$$T_{mx} = \frac{1}{\bar{u}\cdot he}\int_0^h uT\,dy \qquad \text{where } \bar{u} = \int_0^h u\,dy \tag{16}$$

**Table 1.** Parameter combinations

| | $F_c$ | $L_c$ | Re |
|---|---|---|---|
| Case 1 | 0.05 | 0.1 | 500 |
| Case 2 | 0.10 | 0.1 | 500 |
| Case 3 | 0.20 | 0.1 | 500 |
| Case 4 | 0.40 | 0.1 | 500 |
| Case 5 | 0.20 | 0.05 | 500 |
| Case 6 | 0.20 | 0.075 | 500 |
| Case 7 | 0.20 | 0.15 | 500 |
| Case 8 | 0.20 | 0.2 | 500 |
| Case 9 | 0.20 | 0.1 | 100 |
| Case 10 | 0.20 | 0.1 | 1,000 |
| Case 11 | 0.10 | 0.2 | 500 |
| Case 12 | 0.40 | 0.2 | 500 |

The dimensionless variable $\theta_{mX}$ is defined as

$$\theta_{mX} = \frac{T_{mx} - T_0}{T_H - T_0} \tag{17}$$

The local Nusselt number is calculated by the following equation:

$$\mathrm{Nu}_X = \frac{q''_w}{T_H - T_{mx}} \frac{he}{k} = \left( -\frac{\partial \theta}{\partial Y}\bigg|_{Y=\pm 0.5} \right) \frac{1}{1 - \theta_{mX}} \tag{18}$$

The average local Nusselt number from $X_1$ to $X_2$ along the heated surface is expressed as

$$\mathrm{Nu}_{(X_1)-(X_2)} = \frac{1}{|X_2 - X_1|} \int_{X_1}^{X_2} \mathrm{Nu}_X \, dX \tag{19}$$

The time-averaged local Nusselt number per periodic cycle along the heated surface is defined by

$$\overline{\mathrm{Nu}} = -\frac{1}{\tau_p} \int_0^{\tau_p} \mathrm{Nu}_X \, d\tau \qquad \text{where } \tau_p \text{ is time of a periodic cycle} \tag{20}$$

The time-averaged Nusselt number of average local Nusselt number from $X_1$ to $X_2$ along the heated surface per periodic cycle along the heated surface is defined by

$$\overline{\mathrm{Nu}_{(X_1)-(X_2)}} = -\frac{1}{\tau_p} \int_0^{\tau_p} \mathrm{Nu}_{(X_1)-(X_2)} \, d\tau \tag{21}$$

The following equation is used to calculate the average friction factor $f$ of the periodical flow:

$$f = \frac{(-\Delta p/\Delta x) \times he}{\rho u_0^2/2} \tag{22}$$

where the pressure gradient $\Delta p/\Delta x$ is evaluated by the periodic average pressure difference across the channel sections between the distance $(w_2 + w_3)$ of the heated surface.

To match the boundary conditions at the inlet and outlet of the channel mentioned above, the dimensionless lengths from the inlet and outlet to the cylinder are determined by numerical tests and are equal to 10.0 and 50.0, respectively. The length of the heated surface is from $X = -2$ to $X = 20$. To obtain an

optimal computational mesh, three different non uniform distributed elements, which provide a finer element resolution near the cylinder and walls, are used for the mesh tests. Figures 2*a*–2*c* show the velocity and temperature profiles along the line through the center of the cylinder and parallel to the $Y$ axis at steady state under $\mathrm{Re} = 500$, respectively. Based on the results, the computational mesh with 6,700 elements, which corresponds to 20,216 nodes, is used for all cases in this study. In addition, an implicit scheme is employed to deal with the time differential terms of the governing equations. Three different time steps $\Delta\tau = 0.05$, 0.01, and 0.005 under $\mathrm{Re} = 500$, $L_c = 0.1$, and $F_c = 0.2$ are executed for the time-step tests. The variations of the average Nusselt number along the heated surface $\mathrm{Nu}_{(-0.5)-(2)}$ with time step are shown in Figure 2*d*, and the time step $\Delta\tau = 0.01$ is chosen for all cases in this study.



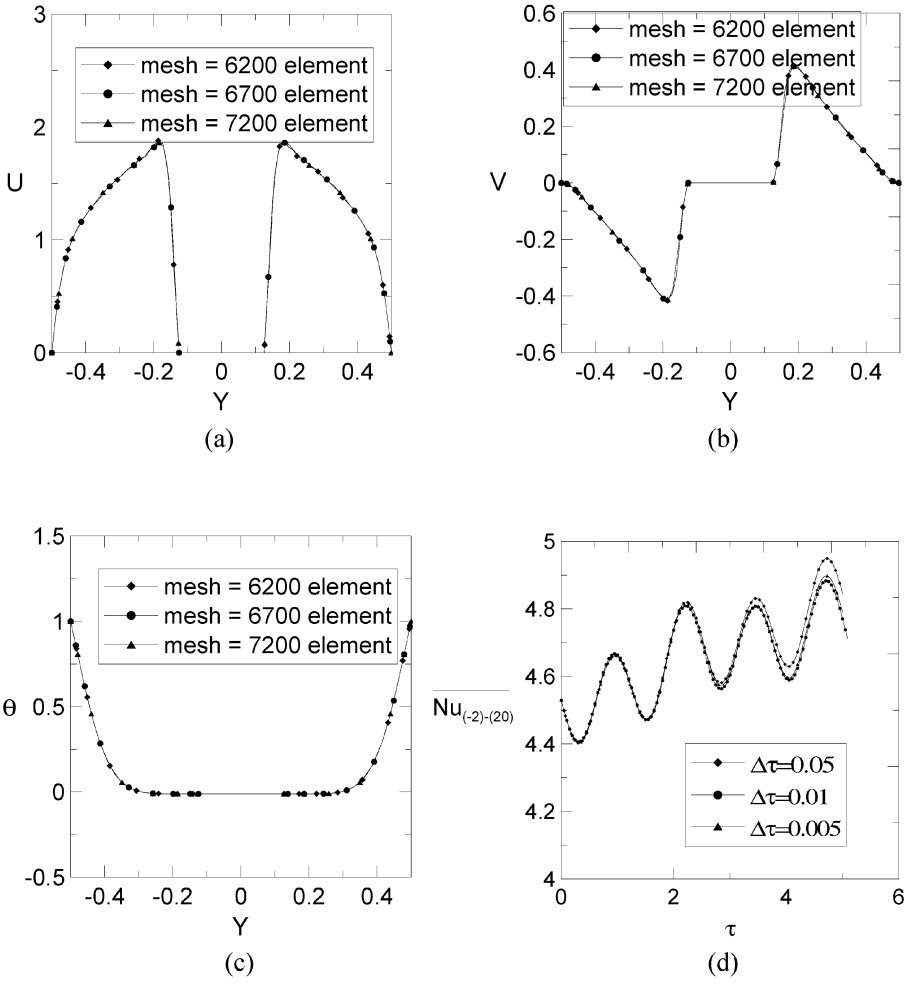


**Figure 2.** Grid and time-step test.

The dimensionless stream function $\Psi$ is defined as

$$U = \frac{\partial \Psi}{\partial Y} \qquad V = -\frac{\partial \Psi}{\partial X} \tag{23}$$

To clearly indicate the phenomena around the moving block, only the flow and thermal fields close to the moving block are illustrated in the following figures. The variations of the streamlines and isothermal lines under $\mathrm{Re} = 500$, $L_c = 0.1$, and $F_c = 0.2$ are indicated in Figures 3 and 4, respectively.

Figure 3 shows the transient developments of the streamlines of case 4. At time $\tau = 0$, the cylinder is stationary and the flow is steady. As shown in Figure 3*a*, the formation of two large symmetric recirculation zones is observed behind the cylinder. As the time $\tau > 0$, the cylinder starts to oscillate with the oscillating velocity $V_c = 2\pi F_c L_c \cos(2\pi F_c \tau)$ and oscillating frequency $F_c = 0.2$. Figures 3*b*–3*g* show the variations of the streamlines during one periodic cycle. In Figure 3*b*, the cylinder moves upward. The fluid near the top region of the cylinder is pressed though the cylinder. Conversely, the fluid near the bottom of the cylinder simultaneously replenishes the vacant space induced by the movement of the cylinder, and forms a recirculation zone due to the continuity of the flow. The cylinder turns downward as it reaches the maximum upper amplitude. As shown in Figure 3*c*, the cylinder is on the way to move downward. Since the moving direction of the cylinder is changed, the fluid near the top region of the cylinder replenishes the vacant space, similar to the phenomenon mentioned above, which causes the recirculation zone around the rear of the cylinder to be shed from the cylinder. Afterward, a new recirculation zone forms around the rear of the cylinder, as shown in Figure 3*d*. In addition, due to the drastic swing of the cylinder, the recirculation zone shed from the cylinder is scattered into the flow gradually. As the cylinder reaches the maximum downward amplitude, the cylinder returns upward immediately, as shown in Figure 3*e*. As in Figure 3*c*, the new recirculation zone is shed from the cylinder, and another recirculation zone is formed around the rear of the cylinder. Finally, the cylinder goes back to the center of the channel and completes a periodic cycle, as shown in Figures 3*f* and 3*g*.

Figure 4 shows the isothermal lines of case 4. Figure 4*a* shows the isothermal lines as the cylinder is stationary. Under the influence of the cylinder, the flow is forced to move toward the wall and depresses the thermal boundary of the heated wall under the cylinder. However, the region affected by the stationary cylinder is small. Figures 4*b*–4*g* show the variations of the isothermal lines during one periodic cycle. Because of the vortex shedding and the oscillating motion of the cylinder, the flow becomes a wavy motion and depresses the thermal boundary of the heated surface intermittently. Then the region affected by the oscillating cylinder becomes larger, which is advantageous to the heat transfer rate of the heated surface.

The distributions of local Nusselt number $\mathrm{Nu}_X$ on the heated wall are shown in Figure 6. The results of the local Nusselt number distribution in the empty channel are the same with the existing study, and the deviations of two results are small, as shown in Figure 5. The situations of the different times in Figure 6 correspond to the those shown in the previous figures. As the cylinder is fixed at the center of the

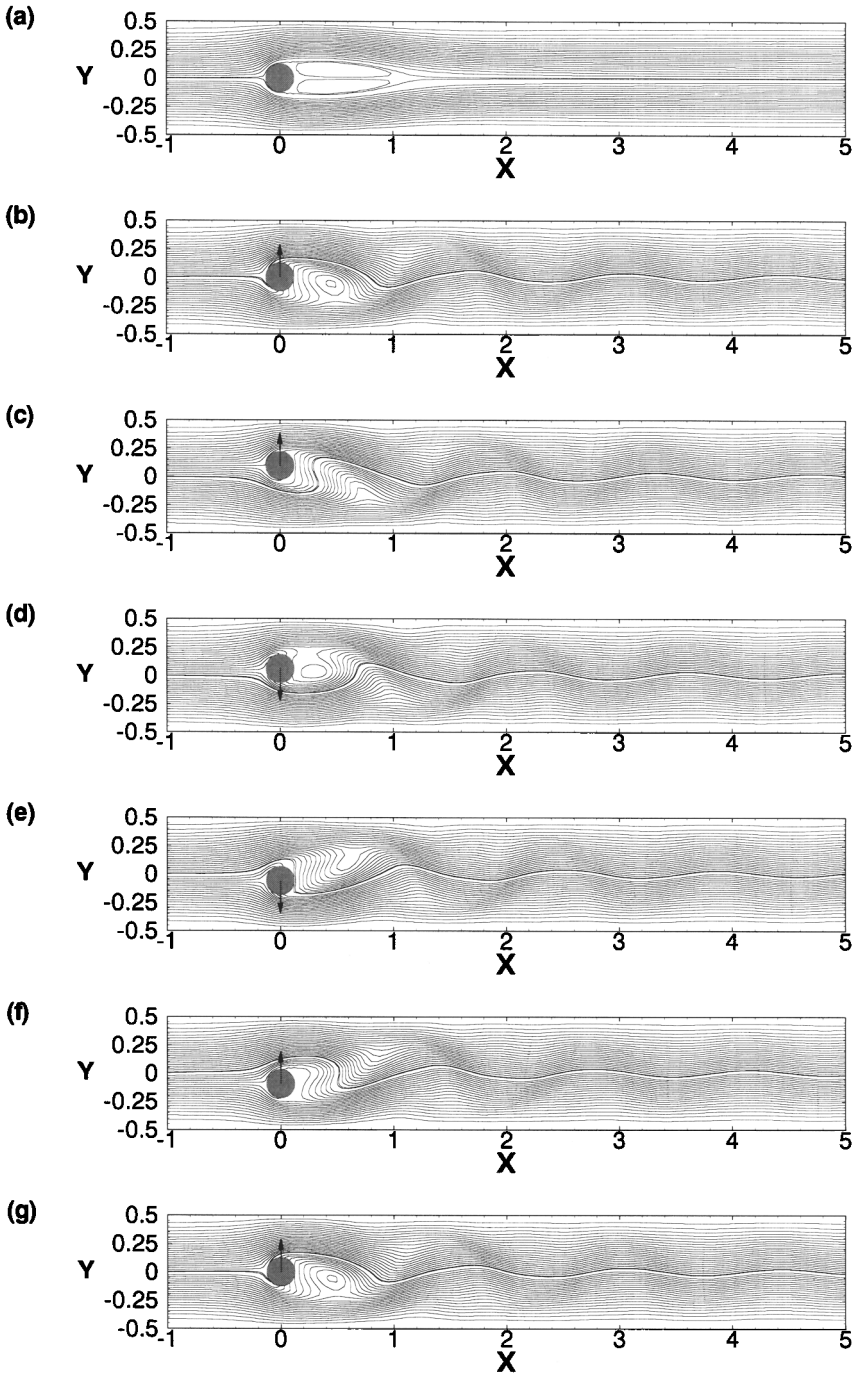


**Figure 3.** Variations of the streamlines during one periodic cycle under case 3.

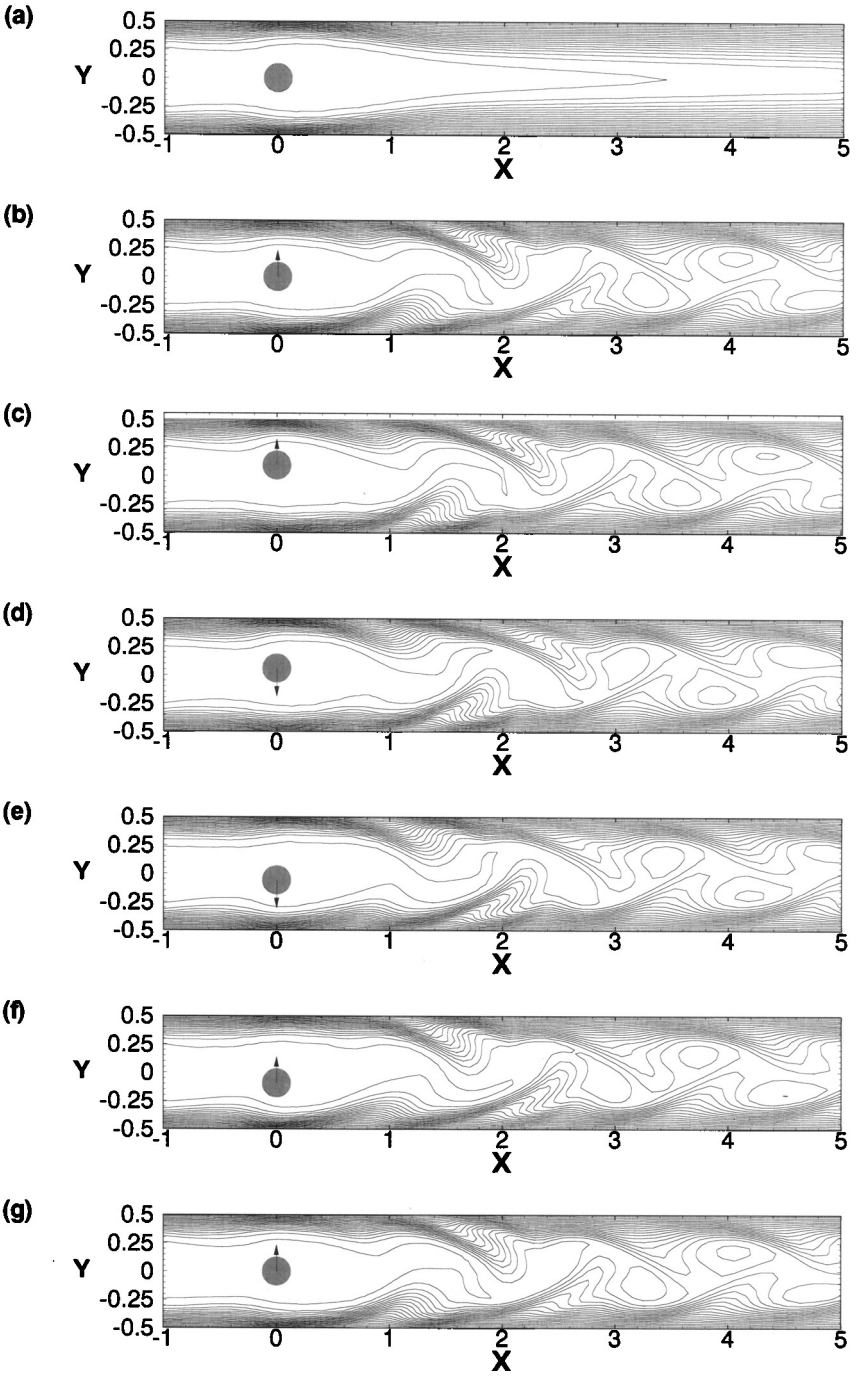


**Figure 4.** Variations of the isothermal lines during one periodic cycle under case 3.

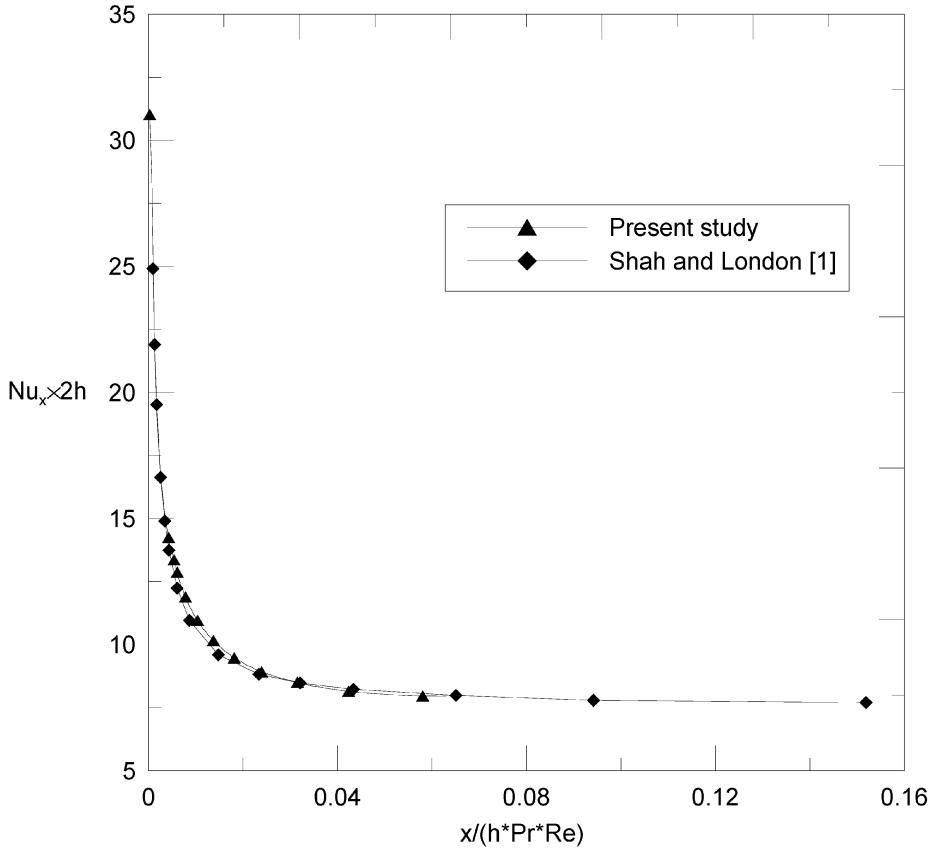


**Figure 5.** Distributions of average Nusselt number along the heated surface with time for case 3.

channel, the flow passing through the cylinder is divided into two equal streams and accelerated, which causes the heat transfer rate of the heated surface close to the cylinder to be enhanced. The local Nusselt numbers near $X = 0$ are larger and vary drastically. The two streams on both sides of the cylinder are symmetric, then after the cylinder the two streams flow steadily and together, which is similar to the flow without insertion of a cylinder. As a result, the vibrations of $\mathrm{Nu}_X$ after $X > 3$ are similar to those of the channel without a cylinder, and decrease monotonically. As the cylinder is oscillating, due to the occurrence of vortex shedding mentioned before, the flow becomes wavy flow and impinges the wall periodically, and disturbs the thermal boundary layer which results in the heat transfer of the heated surface behind the cylinder being enhanced significantly and being larger than that of the stationary cylinder situation. Each time the position of the cylinder shown in the figure is different, which causes the distributions of $\mathrm{Nu}_X$ to be different, too. Except for the former region of heated surface, the cylinder periodically contracts the space on both sides of the cylinder; the value of $\mathrm{Nu}_X$ is then extremely large at the position $(X = 0)$, just under the cylinder. After the cylinder, due to the motion of wavy flow, the distribution of $\mathrm{Nu}_X$ at each time varies in a wavy manner. About $X > 6$, the

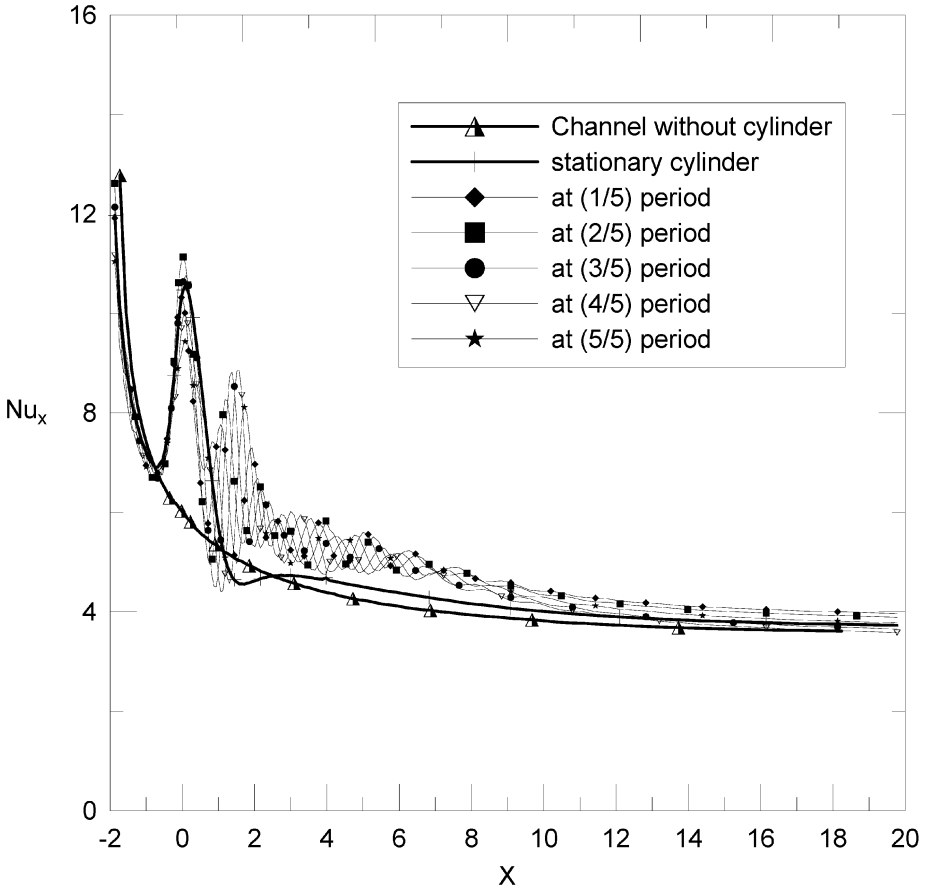


**Figure 6.** Comparison of the local Nusselt number in empty channel with those of existing studies.

**Table 2.** Comparison of the average local Nusselt number $\overline{\mathrm{Nu}_{(x_1)-(x_2)}}$ from $X_1$ to $X_2$ along the heated surface of the cylinder set in the channel with those of the channel without cylinder

| | $X_1 = -0.5$ to $X_2 = 0.5$ | $X_1 = -0.5$ to $X_2 = 2$ | $X_1 = -0.5$ to $X_2 = 5$ | $X_1 = -0.5$ to $X_2 = 10$ |
|---|---|---|---|---|
| (*a*) $\overline{\mathrm{Nu}_{(x_1)-(x_2)}}$ in the channel without cylinder | 6.8 | 5.617 | 4.967 | 4.532 |
| (*b*) $\overline{\mathrm{Nu}_{(x_1)-(x_2)}}$ in the channel with stationary cylinder | 9.62 | 7.041 | 5.824 | 5.050 |
| (*c*) $\overline{\mathrm{Nu}_{(x_1)-(x_2)}}$ in the channel with oscillating cylinder (case 3) | 9.43 | 7.377 | 6.409 | 5.581 |
| $\frac{(b)-(a)}{(a)} \times 100\%$ | 41.40% | 25.36% | 17.25% | 11.41% |
| $\frac{(c)-(a)}{(a)} \times 100\%$ | 38.68% | 31.34% | 29.00% | 23.15% |

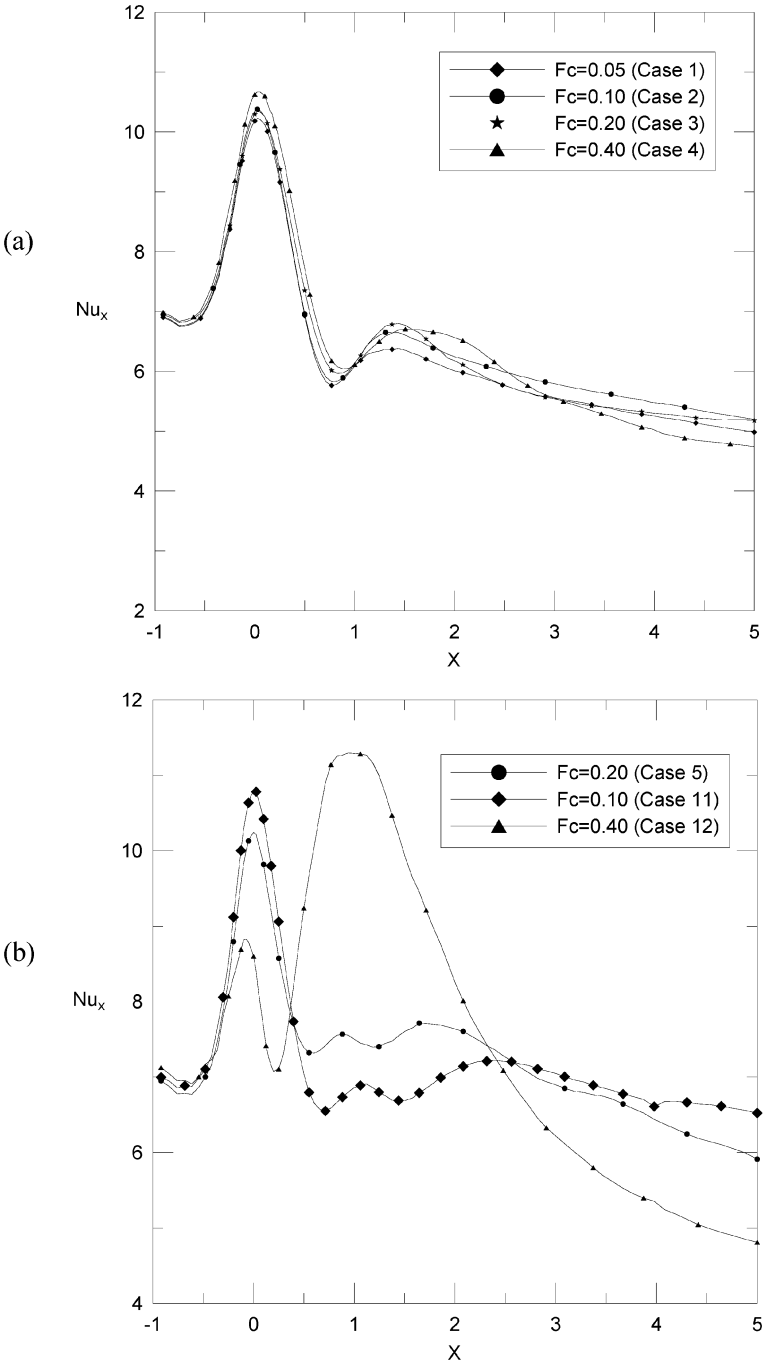


**Figure 7.** Variations of local Nusselt number along the heated surface for different oscillating frequencies under $\mathrm{Re} = 500$, (*a*) $L_c = 0.1$, (*b*) $L_c = 0.2$.

variations of the distributions of $Nu_X$ become flat, but the values of $Nu_X$ are still larger than those of the channel without a cylinder and with a stationary cylinder.

The comparison of the time-average Nusselt numbers of the average local Nusselt numbers ($\overline{Nu_{(X_1)-(X_2)}}$) among stationary and oscillating cylinders and the channel without a cylinder are shown in Table 2. When the region is far away from the cylinder, the influence of the cylinder on the local Nusselt number decreases, so the average local Nusselt number decreases accompanying the farther downstream region. Therefore, the enhancement of heat transfer relative to the channel without a cylinder is monotonically decreased as the region covers the farther downstream region. Except for the region just under the cylinder ($X_1 = -0.5$ to $X_1 = 0.5$), the enhancements of heat transfer of the oscillating cylinder cases are superior to those of the stationary cylinder case. These results could indicate how long the region could be used effectively.

Figure 7 shows the variations of local Nusselt number $Nu_X$ of the cylinder with time for different oscillating frequencies under $Re = 500$. The definition of the

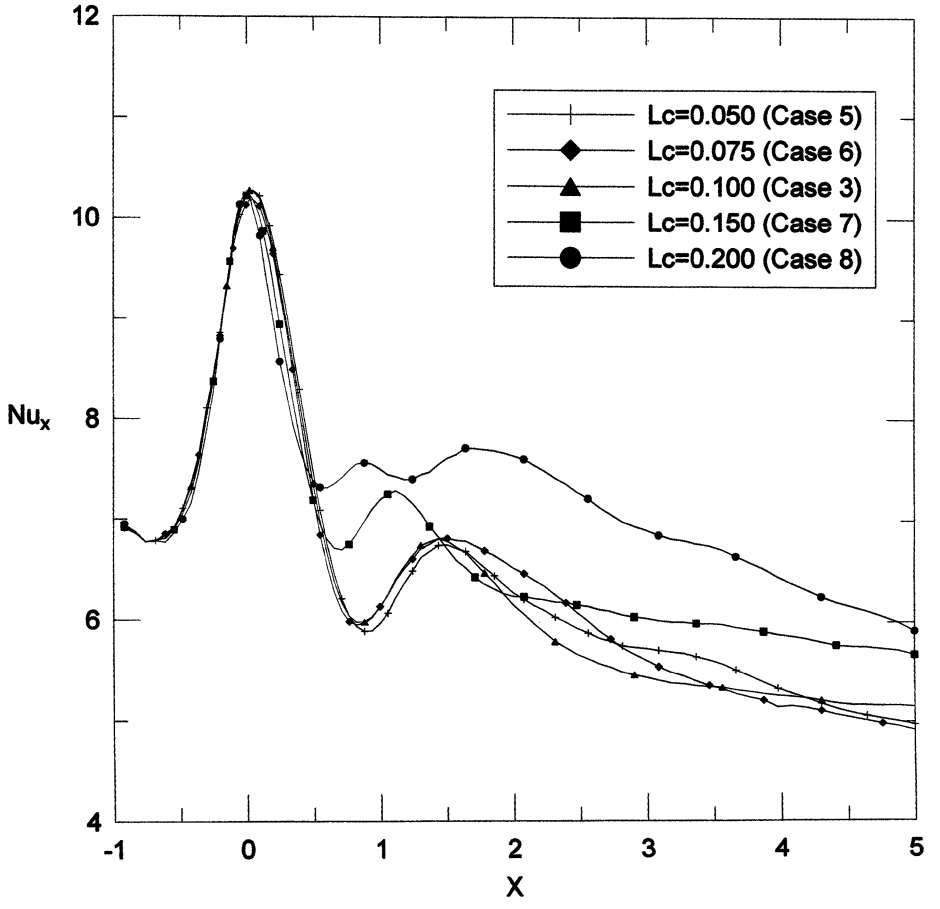


**Figure 8.** Variations of local Nusselt number along the heated surface for different oscillating amplitude under $Re = 500$ and $F_c = 0.2$.

dimensionless frequency in this study is the same as the Strouhal number defined in the other studies. In Figure 7*a*, the oscillating amplitude $L_c$ is 0.1. The difference among these cases is not apparent. The small amplitude of $L_c$ is suggested as a main reason. As the oscillating amplitude increase to 0.2, the effect of the oscillating frequency on the heat transfer rate of the heated wall becomes remarkable, as shown in Figure 7*b*. When the cylinder oscillates at higher frequency ($F_c = 0.4$), the cylinder oscillates at higher velocity for the same amplitude, which could cause the wavy motion of flow behind the cylinder to be more violent and increase the heat transfer rate on the heated wall behind the cylinder substantially. The summit value occurs near the position ($X = 1$) behind the cylinder, not just under the cylinder; this phenomenon is rather different from the other cases. Furthermore, the above phenomenon is different from those of the cylinder oscillating in board space [13–15], in which the natural frequency is about 0.2. The reason is supposed that the flow is essentially restricted to walls.



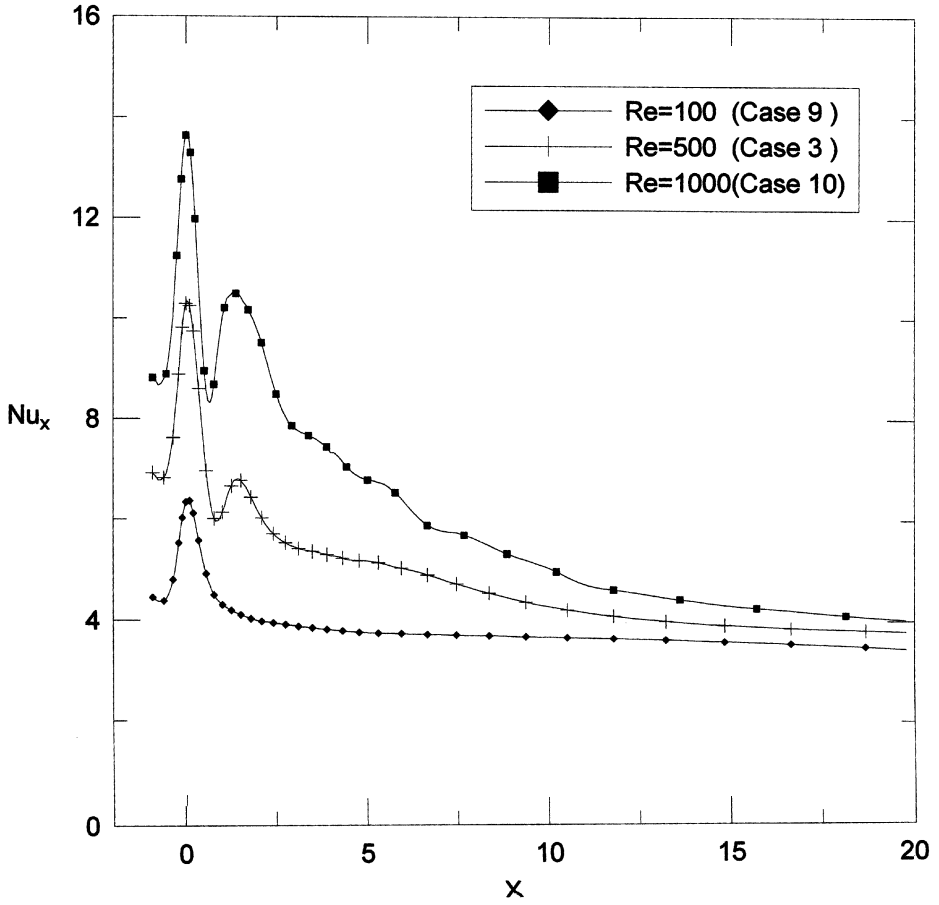


**Figure 9.** Variations of local Nusselt number along the heated surface for various Reynolds numbers under $F_c = 0.2$ and $L_c = 0.1$.

**Table 3.** Thermal performance under constant pumping power condition

| $F_c$ | $L_c$ | Re | Thermal performance $(\overline{\mathrm{Nu}_{(-2)-(20)}}/\overline{\mathrm{Nu}_e})/(f/f_e)^{1/3}$ |
|---|---|---|---|
| 0.05 | 0.1 | 500 | 0.9524 |
| 0.10 | 0.1 | 500 | 0.9660 |
| 0.20 | 0.1 | 500 | 0.9410 |
| 0.40 | 0.1 | 500 | 0.8661 |
| 0.20 | 0.05 | 500 | 0.9512 |
| 0.20 | 0.2 | 500 | 0.9365 |
| 0.20 | 0.1 | 100 | 0.9303 |
| 0.20 | 0.1 | 1,000 | 0.9700 |



The effects of the oscillating amplitude on the heat transfer are shown in Figure 8 for $\mathrm{Re} = 500$ and $F_c = 0.2$. As the oscillating amplitude of the cylinder increases, the flow is disturbed more drastically, which makes the variation of the flow more apparent. Consequently, the heat transfer rate is enhanced remarkably with increment of the oscillating amplitude. However, as the oscillating amplitude is lower than 0.1, the variation of the heat transfer rate becomes flat.

The effects of the Reynolds number on the heat transfer are shown in Figure 9 for the $L_c = 0.1$ and $F_c = 0.2$ situation. The higher the Reynolds number, quicker and more drastic are the velocity and disturbance of fluid, respectively. Then the heat transfer rate is enhanced remarkably with increment of the Reynolds number. At low Reynolds number ($\mathrm{Re} = 100$), it is hard to form periodic wake and vortex sheets, so the heat transfer rate is almost the same as that of the channel with a stationary cylinder.

The criterion of $(\overline{\mathrm{Nu}_{(-2)-(20)}}/\overline{\mathrm{Nu}_e})/(f/f_e)^{1/3}$, the thermal performance of the heat transfer under constant pumping power constraint, was suggested by Webb and Eckert [22] and Han et al. [23]. Table 3 shows the thermal performance under constant pumping power condition for some cases in this study, and the results are close to 1.

## CONCLUSIONS

The heat transfer characteristics of a heated wall in a channel with a transversely oscillating cylinder in cross-flow are investigated numerically. Some conclusions are summarized as follows.

1. The heat transfer rate of the cylinder oscillating in the channel is better than that of the channel without a cyclinder. Comparing with the stationary cylinder in the channel, the cylinder oscillating in the channel forms wavy flow which could improve the heat transfer substantially behind the cylinder.
2. The influence of oscillating frequency on the heat transfer rate is not obvious as the oscillating amplitude is small. When the oscilliating frequency increases, the heat transfer rate under the cylinder and the influential range decrease, but the heat transfer rate behind the cylinder increases substantially.

3. The heat transfer rate is increased drastically when the oscillating amplitude of the cylinder and the Reynolds number are increased.

## REFERENCES


1. R. K. Shah and A. L. London, *Laminar Flow Forced Convection in Ducts*, Academic Press, New York, 1978.
2. E. M. Sparrow, J. E. Nithammer, and A. Chaboki, Heat Transfer and Pressure Drop Characteristics of Arrays of Rectangular Modules Encountered in Equipment, *Int. J. Heat Mass Transfer*, vol. 25, no. 7, pp. 961–973, 1982.
3. G. Bergeles and N. Athanassiadis, The Flow Past a Surface-Mounted Obstacle, *J. Fluids Eng.*, vol. 105, pp. 461–463, 1983.
4. T. M. Liou, Y. Chang, and D. W. Hwang, Experimental and Computational Study of Turbulent Flows in a Channel with Two Pairs of Turbulence Promoters in Tandem, *J. Fluids Eng.*, vol. 112, pp. 302–310, 1990.
5. T. M. Liou, W. B. Wang, and Y. J. Chang, Holographic Interferometry Study of Spatially Periodic Heat Transfer in a Channel with Ribs Detached from One Wall, *Trans. ASME*, vol. 117, p. 199, 1995.
6. J. J. Hwang and T. M. Liou, Heat Transfer in a Rectangular Channel with Perforated Turbulence Promoters Using Holographic Interferometry Measurement, *Int. J. Heat Mass Transfer*, vol. 38, no. 17, pp. 3197–3207, 1995.
7. C. H. Amon and B. B. Mikic, Numerical Prediction of Convective Heat Transfer in Self-sustained Oscillatory Flows, *J. Thermophys. Heat Transfer*, vol. 4, no. 2, pp. 239–246, 1990.
8. D. Majumdar and C. H. Amon, Heat and Momentum Transport in Self-sustained Oscillatory Viscous Flows, *Trans. ASME, J. Heat Transfer*, vol. 114, no. 4, pp. 866–873, 1992.
9. H. H. Lin and Y. H. Hung, Transient Forced Convection Heat Transfer in a Vertical Rib-Heated Channel Using a Turbulence Promoter, *Int. J. Heat Mass Transfer*, vol. 36, no. 6, pp. 1553–1571, 1993.
10. J. J. Hwang, Heat Transfer-Friction Characteristic Comparison in Rectangular Ducts with Slit and Solid Ribs Mounted on One Wall, *Trans. ASME, J. Heat Transfer*, vol. 120, pp. 709–716, 1998.
11. H. W. Wu and S. W. Perng, Effect of an Oblique Plate on the Heat Transfer Enhancement of Mixed Convection over Heated Blocks in a Horizontal Channel, *Int. J. Heat Mass Transfer*, vol. 42, pp. 1217–1235, 1999.
12. Wu-Shung Fu, Wen-Wang Ke, and Ke-Nan Wang, Laminar Forced Convection in a Channel with a Moving Block, *Int. J. Heat Mass Transfer*, vol. 44, no. 13, pp. 2385–2394, 2001.
13. R. Chilukuri, Incompressible Laminar Flow Past a Transversely Vibrating Cylinder, *J. Fluids Eng.*, vol. 109, pp. 166–171, 1987.
14. M. O. Griffin and M. S. Hall, Review—Vortex Shedding Lock-on and Flow Control in Bluff Body Wakes, *J. Fluids Eng.* vol. 113, pp. 526–537, 1991.
15. Jianfeng Zhang and Charles Dalton, Interaction of a Steady Approach Flow and a Circular Cylinder Undergoing Forced Oscillation, *J. Fluids Eng.* vol. 119, pp. 808–813, 1997.
16. C.-H. Cheng, H.-N. Chen, and W. Aung, Experimental Study of the Effect of Transverse Oscillation on Convection Heat Transfer from a Circular Cylinder, *J. Heat Transfer*, vol. 119, pp. 474–482, 1997.
17. C.-H. Cheng, J.-L Hong, and W. Aung, Numerical Prediction of Lock-on Effect on Convective Heat Transfer from a Transversely Oscillating Circular Cylinder, *Int. J. Heat Mass Transfer*, vol. 40, pp. 1825–1834, 1997.

18. D. Karanth, G. W. Rankin, and K. Sridhar, A Finite Difference Calculation of Forced Convective Heat Transfer from an Oscillating Cylinder, *Int. J. Head Mass Transfer*, vol. 37, pp. 1619–1630, 1994.
19. C. Gau, J. M. Wu, and C. Y. Liang, Heat Transfer Enhancement and Vortex Flow Structure over a Heated Cylinder Oscillating in the Crossflow Direction, *J. Heat Transfer*, vol. 121, pp. 789–795, 1999.
20. H. G. Park and M. Gharib, Experimental Study of Heat Convection from Stationary and Oscillating Circular Cylinder in Cross Flow, *Trans. ASME, J. Heat Transfer*, vol. 123, no. 1, pp. 51–62, 2001.
21. W. S. Fu and S. J. Yang, Numerical Simulation of Heat Transfer Induced by a Body Moving in the Same Direction as Flowing Fluids, *Int. J. Heat Mass Transfer*, vol. 36, pp. 257–264, 2000.
22. R. L. Webb, E. R. C. Eckert, and R. J. Goldstein, Heat Transfer and Friction in Tubes with Repeated-Ribs Roughness, *Int. J. Heat Mass Transfer*, vol. 14, pp. 1647–1658, 1972.
23. J. C. Han, L. R. Glicksman, and C. K. Lei, Heat Transfer Enhancement in Channels with Turbulence Promoters, *Trans, ASME, J. Heat Transfer* vol. 21, pp. 628–635, 1985.